Whispering galleries modeling

Didier Cassereau[1], Vincent Gibiat[2] and Pierre de Guibert[2]

[1] *Laboratoire d'Imagerie Biomédicale, 15 rue de l'Ecole de Médecine, 75006 Paris, France*

[2] *Laboratoire PHASE, Université Paul Sabatier, 118 route de Narbonne, 31062 Toulouse cedex 9, France*

Abstract

The whispering galleries phenomenon can be observed at various locations in the world, like the main dom of the St-Paul cathedral in London. Various physical interpretations of this phenomenon have been suggested by Lord Airy and Lord Rayleigh in the XIXth century, based on either multiple reflections of a wave in air or on surface waves that travel along the solid interface of the dom.
In this work, we present various numerical simulations that can help understanding the propagation of a surface wave inside the solid layer that surrounds the volume of the dom. In particular we can observe how the incident energy is mainly trapped inside the solid shell. Measurements have been realised with a semi-closed cavity made of a 5cm-thick curved plasterboard, with microphones located at different positions near the wall.
We present comparisons between experimental and numerical results, helpful to better understand the complexity of the measured signals.

Introduction

The whispering galleries phenomenon is a quite surprising acoustic phenomenon that can be observed at various locations in the world, like the main dome of the St-Paul cathedral in London: walking just under the dome, it is possible to whisper near the wall ; another visitor, located at a completely different location under the dome, can under some circumstances hear what we have whispered, although the large distance (40-50m) between the two persons. Here we can mention some other famous locations in the world, where this kind of phenomenon can be observed: the Tabernacle in Salt Lake City (Mormon monument), the Galerie des Cariatides at the Louvre museum in Paris, or the Chaise-Dieu Abbey (Auvergne, France). A similar acoustic phenomenon can also be observed in some metro stations.

A common feature of these various locations is that we consider an acoustic source located inside a reflecting and concave cavity.

In this paper, we propose a numerical modelling of this phenomenon, with experimental measurements realised at a reduced scale. This allows to illustrate the existence of surface waves that travel along the wall. These surface waves can permanently radiate in direction of the inside of the cavity, and can consequently explain the whispering galleries phenomenon.

A few historical reminders

The whispering galleries phenomenon has been observed at the end of the XIX$^{\text{th}}$ century under the dome of the St-Paul cathedral in London:

- 1871: Lord Airy, Astronomer Royal of the Great Britain Court (1835-1881), provides a physical interpretation in terms of geometrical acoustics, including multiple reflections of the signal on the walls of the concave cavity,
- 1896: Lord Rayleigh disputes Airy's interpretation and gives his own explanation in terms of modal propagation inside the volume, associated with surface waves that propagate along the wall,
- 1904, 1910: Rayleigh realizes an experimental measurement at a reduced scale in his laboratory,
- 1922: Raman and Sutherland confirm Rayleigh's interpretation.

One of the fundamental questions that arises from this work is the following: what can we really measure in an experiment like Rayleigh's experiment? Nowadays, the available experimental equipments are significantly more efficient than at the beginning of the XX$^{\text{th}}$ century. We now also have the possibility to run numerical simulations to try to understand the phenomenon.

Rayleigh's experiment

The Rayleigh's experiment, at the beginning of the XX$^{\text{th}}$ century, is illustrated by Figure 1. It uses a thin cylindrical metallic plate of diameter 2m. The source is a bird call (B) that mainly behaves as a small organ pipe, with a frequency near 4kHz, and a sensitive flame (F) is used as detector. As a preliminary step for this experiment, it has been verified that no direct sound, from the source to the detector, could be detected by the sensitive flame.

A first measurement is done using a free metallic plate: the sensitive flame flickers, revealing the existence of a vibration in air. Then, a second measurement is done by adding an obturating screen (W) on the metallic plate: the sensitive flame does not show any movement.

The interpretation given by Rayleigh to these observations is based on a surface wave that propagates along the metallic plate and permanently radiates back in air. In the presence of the obturating screen, this surface wave cannot reach the sensitive flame, therefore resulting in the absence of any movement. It results therefore that this experiment, realized at a reduced scale, *a priori* con-

firms Rayleigh's assumption, instead of Airy's explanation.

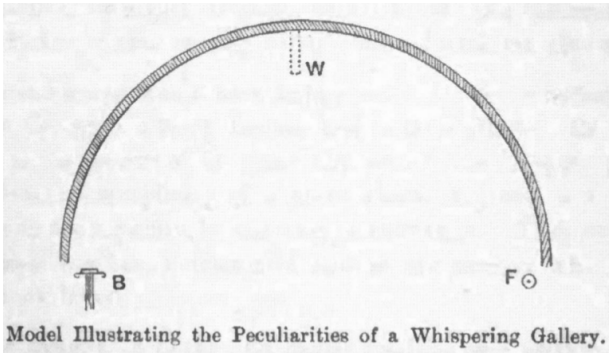

Figure 1: Rayleigh's experiment.

Numerical modeling

The numerical modeling is based on the two-dimensional FDTD (Finite Differences Time Domain) code SimSonic. The configuration of the numerical simulation is illustrated by Figure 2.

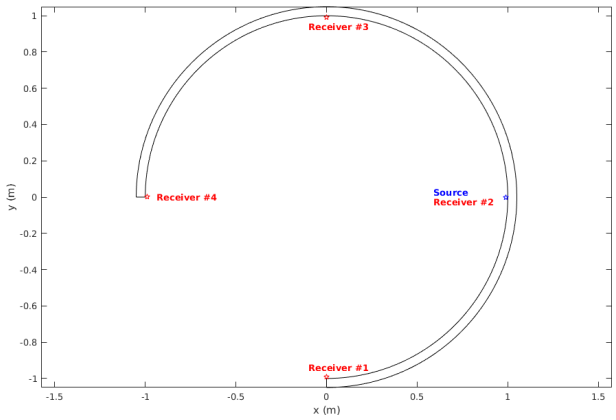

Figure 2: Configuration of the numerical model.

The wall closing the cavity is a partially opened plaster cylinder of diameter 2m and thickness 5cm. The inside and outside of the plaster cylinder are filled with air.

A point-like source is located at the position illustrated in blue on Figure 2, at a distance of 5cm from the wall. This source generates a gaussian pulse with a central frequency of 4kHz. Four receivers are located at 1cm from the wall, at four different locations illustrated in red.

The mechanical properties of air and plaster are the following:

- air: c=340 m/s, ρ_a=1.2 kg/m^3
- plaster: c_l=2400 m/s, c_t=1500 m/s, ρ_p=2790 kg/m^3

Figure 3 illustrates snapshots of the acoustic field at four different observation times:

- on Figure 3a (t=0.7ms), we clearly identify the incident wavefront (that propagates from the source to the top of the figure), as well as the wavefront reflected by the bottom wall ; as the distance between the source and the wall is very small, these two wavefronts cannot be really distinguished ; we can also observe the existence of a faster wave inside the plaster shell,
- on Figure 3b (t=2.5ms), the bulk wave in air grows, and the faster wave in plaster continues ahead,
- Figures 3c and 3d illustrate the temporal evolution of these various effects.

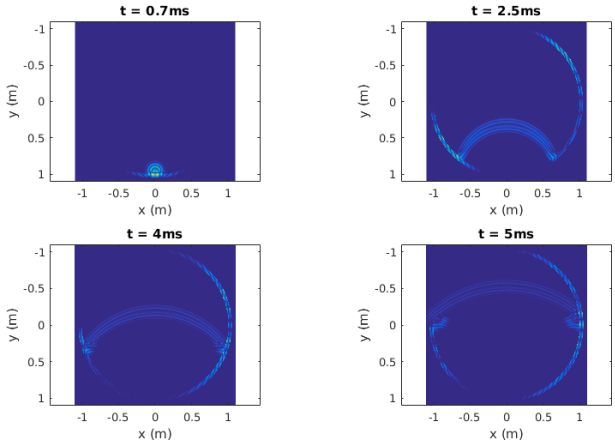

Figure 3: Instantaneous snapshots of the field.

After some time, we can observe that an important part of the energy is trapped in the plaster shell, propagating from one end of the structure to the other one and back. We can also note that this fast wave radiates permanently in the air inside the cavity.

Figure 4 represents the temporal signal measured by each receiver. In the four cases we can observe some complex signals, with various components arriving at different times (coda). The first signal on Figure 4b (top/right) corresponds to the direct wave in air (the receiver is located just in front of the source). Similarly the first signal on Figures 4a (top/left) and 4c (bottom/left) corresponds to the same direct wave in air that propagates from the source to the receivers, turned of $\pm 90°$ with respect to the source position. Finally, we clearly see on Figure 4d two different pulses, that both correspond on the bulk wave in air, the first one corresponding to the direct propagation from the source to the receiver, and the second one coming from a reflection on the wall, refocused inside the cavity due to the concavity of the surface.

On Figure 5 we have represented the same four temporal signals, but limited to a zoom of the temporal part that immediately precedes the first arriving signal. For the second receiver that is located just in front of the source, we do not observe anything. But the signals measured by receivers #1, #3 and #4 clearly contain an additional component, whose apparent frequency is smaller, of very small amplitude (typically 1‰ of the amplitude of the direct wave in air), and corresponding to a larger wave velocity than in air.

The same computation has been made, with multiple receivers all along the wall, at a distance of 1cm from

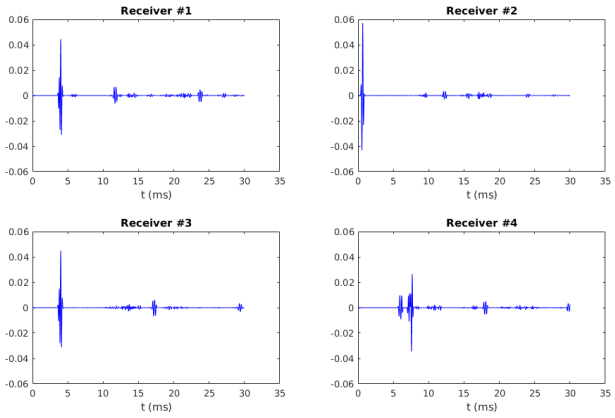

Figure 4: Temporal signals measured by the receivers.

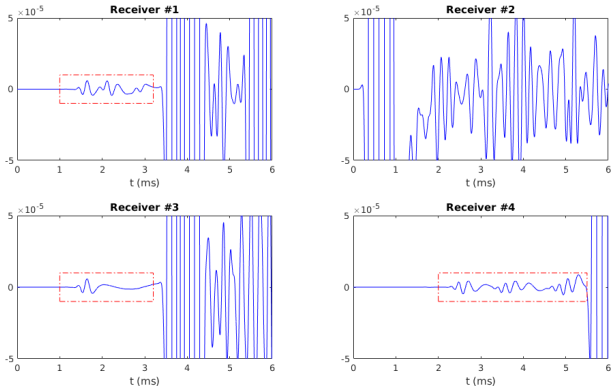

Figure 5: Zoom just before the first arriving signal.

the wall. The obtained result is illustrated on Figure 6 through a space/time representation in log scale.

Here we can clearly see the main curved wavefront that simply corresponds to the direct wave in air from the source to the different receivers. A simple geometrical analysis allows to understand the curvature of this wavefront, due to the distance between the source and the receivers that depends on the angle between the source and each receiver.

After this main wavefront we can identify the complex temporal structure of the coda, mixing direct and reflected waves propagating in air, and radiation of the wave in plaster back in air.

On this figure we can also observe a contribution before the first direct wave, therefore corresponding to a larger propagation velocity. The relationship between arrival time and position of the receiver appears strictly linear. As the receivers are represented by their angle with respect of the source, this linearity can be only explained by a wave that propagates along the curved surface of the plaster wall.

The slope, illustrated by the dashed line, allows to evaluate the equivalent propagation velocity. We obtained a value of about 1286m/s, thus a velocity that is smaller but similar to the transverse velocity in plaster (this is coherent with the assumption of a Rayleigh wave).

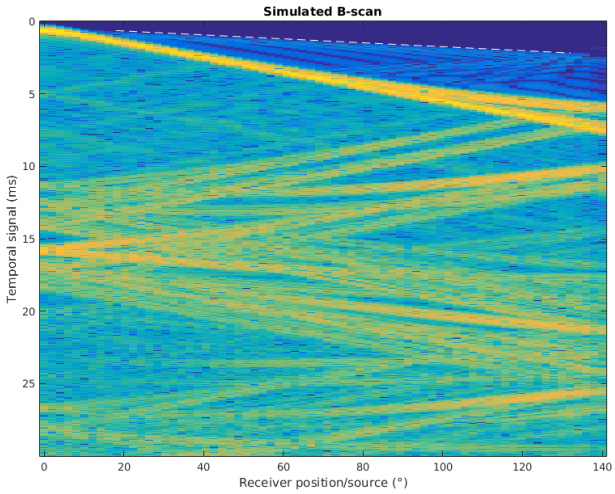

Figure 6: Space/time representation for multiple receivers.

Experimental measurements

An experimental setup has been designed, similar to the numerical model presented in the previous section. This setup is illustrated on Figures 7 (general view of the experiment) and 8 (detailed view, including the source and a set of 4 receivers that can be moved along the perimeter of the plaster wall).

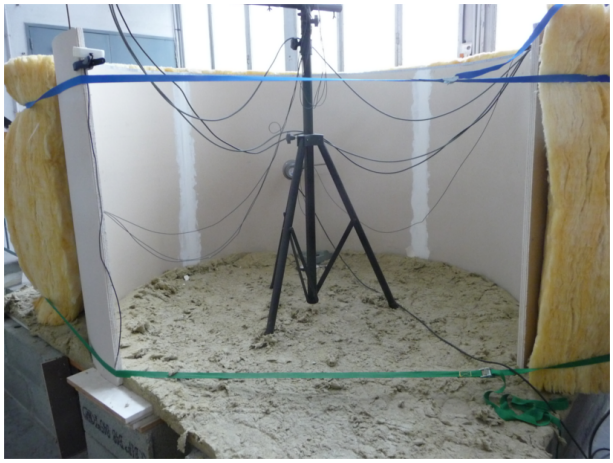

Figure 7: Global view of the experimental setup.

The experimental measurements are illustrated on Figure 9 through a space/time representation. On this figure we clearly see the main and curved wavefront that corresponds to the direct wave in air, also observed in the numerical simulation. We also see the complex coda after the first arriving signal.

Figures 10a (top/left) and 10b (top/right) represent the temporal signals measured at two particular positions of the receivers: just in front of the source (10a) and at a distance of 64mm (10b). Figures 10c (bottom/left) and 10d (bottom/right) represent a zoom of these two signals, restricted to the part that immediately precedes the arrival of the direct wave.

Except the very low frequency component that corresponds to measurement noise (∼50Hz), we do not observe

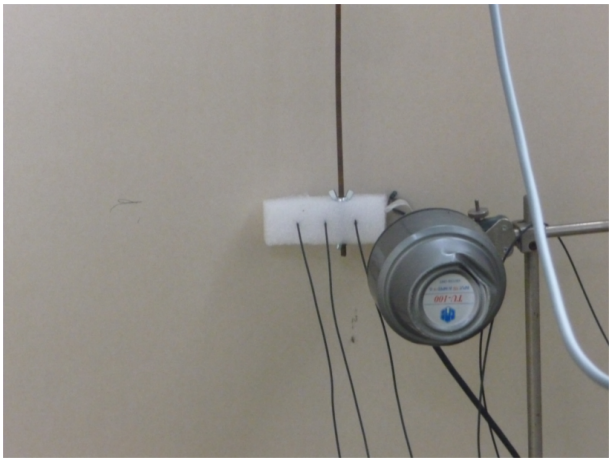

Figure 8: Detailed view of the experimental setup.

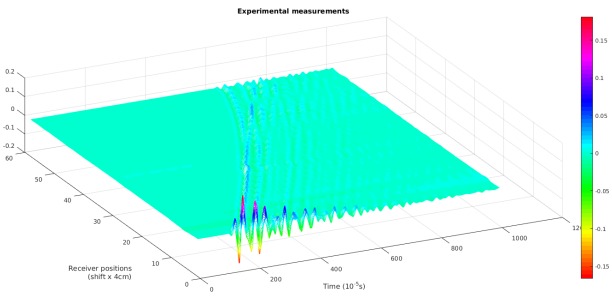

Figure 9: Experimental measurements, in a space/time representation.

any fast wave component for the first receiver located just in front of the source. But for the second receiver at 64mm from the source, we clearly see a small signal. These measurements confirm the numerical results presented in the previous section.

Conclusion

As a first conclusion, it clearly appears from numerical simulations and experimental measurements that the temporal signals are very complex, with multiple contributions coming from direct and reflected waves in air (reflected waves are refocused inside the cavity due to the concave curvature of the wall). The experimental measurement is really a challenge as the measurement is perturbed by the ambiant noise and measurement conditions. It is also remarkable that the effect we want to measure is very small, making its experimental detection more difficult.

In this work, we also illustrated the existence of a fast wave radiating in the fluid, that can be interpreted as a surface wave that propagates along the wall of the cavity. Numerically it is not very difficult to observe this effect, but experimentally it is significantly more complex.

We still have to improve the experimental setup, and run some additional numerical simulations, in order to better understand the complex physical phenomena that are involved in this problem.

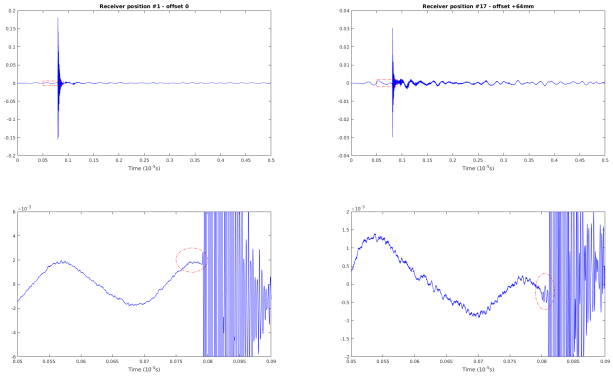

Figure 10: Temporal signals measured at two particular positions of the receivers.

References

[1] G. B. Airy, *On Sound and Atmospheric Vibrations, with the Mathematical Elements of Music* (London, MacMillan), p. 145 (1871),

[2] J. W. Strutt, Baron Rayleigh, *On the Whispering Galleries* in *Theory of Sound* **2**, pp. 127-129 (1896),

[3] J. W. Strutt, Baron Rayleigh, *The Problem of the Whispering Gallery*, Philosophical Magazine **20**, pp. 1001-1004 (1910),

[4] J. W. Strutt, Baron Rayleigh, *On shadows*, Royal Institution Proceedings (1904),

[5] J. W. Strutt, Baron Rayleigh, *Further Applications of Bessel's Functions of High Order to the Whispering Gallery and Allied Problems*, Philosophical Magazine **xxvii**, pp. 100-109 (1914),

[6] C. V. Raman and G. A. Sutherland, *On the Whispering-Gallery Phenomenon*, Proceedings of the Royal Society of London, Series A, 100, No. 705, pp. 424-428 (1922),

[7] H. G. Dorsey, *Acoustics of Arches*, J. Acoust. Soc. Am. **20**, p. 597 (1948),

[8] W. C. Sabine, *Collected papers on acoustics*, Cambridge Harvard University, pp. 255-269 (1922),

[9] E. Bossy, http://www.simsonic.fr.